Opto-Electronics Review

journal homepage: https://journals.pan.pl/opelre

Simulation of the efficiency dependency of multi-junction photovoltaic cells based on titanium oxide and copper oxide using SCAPS software

Grzegorz Wisz[1], Mirosław Łabuz[2*], Mariusz Bester[2], Andrzej Wal[2]

[1] Institute of Materials Engineering, Faculty of Exact and Technical Sciences, University of Rzeszów, ul. Stanisława Pigonia 1, 35-310 Rzeszów, Poland
[2] Institute of Physics, Faculty of Exact and Technical Sciences, University of Rzeszów, ul. Stanisława Pigonia 1, 35-310 Rzeszów, Poland

Article info

Article history:
Received 30 Oct. 2025
Received in revised form 05 Feb. 2026
Accepted 10 Feb. 2026
Available on-line 14 Apr. 2026

Keywords:
TiO_2/Cu_xO;
thin film;
solar cells;
SCAPS simulation.

Abstract

To advance the development of thin-film photovoltaic (PV) technologies, current research is increasingly focused on identifying alternative materials to zinc oxide (ZnO), cadmium sulfide (CdS), cadmium telluride (CdTe), and copper indium gallium selenide (CIGS). Among the most promising candidates are titanium oxide (TiO_2) and copper oxide (Cu_2O or CuO), owing to their abundance, non-toxicity, and favourable optoelectronic properties. This study presents a simulation-based investigation of a multi-junction PV structure based on n-TiO_2/p-Cu_xO single cell using the solar cell capacitance simulator (SCAPS). The multi-junction configuration offers significant efficiency advantages over single-junction cells by minimising defects associated with lattice mismatch for thinner TiO_2/Cu_xO layers in a tandem device. Reducing interface defect density through improved fabrication techniques could substantially enhance efficiency. Furthermore, in multi-junction architectures, improved carrier extraction and reduced recombination losses increase the open-circuit voltage (V_{oc}), thereby improving carrier transport to external contacts and enhancing cell performance.

1. Introduction

Recent research has turned toward the development of multi-junction structures, which can significantly enhance energy conversion by utilizing a broader spectrum of sunlight and mitigating recombination losses. Multi-junction cells, by stacking materials with different band gaps, allow for more efficient photon absorption and better charge separation. Among the materials being investigated for solar cell production, TiO_2 and Cu_xO (cupric oxide – CuO and cuprous oxide – Cu_2O) are widely used due to their features, such as low production cost, low power consumption, ease of synthesis, and high theoretical efficiency [1–4]. Incorporating TiO_2 and Cu_xO in a multi-junction configuration could overcome the limitations of single-junction devices, particularly those caused by lattice mismatch and interface defect densities. The development of current thin-film solar cells focuses on new structures that primarily enable reduced production costs and increased cell efficiency. However, implementing all new ideas in the laboratory and evaluating the results is unnecessary and a waste of time. Therefore, it seems reasonable to use tools that allow numerical simulations, enabling the "construction" and optimisation of solar cell performance, followed by physical testing of the most promising solutions. At present, researchers use a range of tools to simulate thin-film solar cells, depending on the problem complexity, application context, and expected outcomes [5–6]. The aim of our paper was to simulate TiO_2/Cu_xO multi-junction solar cells [7–10] and among several most popular simulation programs for such a type of junctions are the following tools: ADEPT [11, 12], AFORS-HET [13, 14], AMPS [15, 16], PC1D [17, 18], SCAPS [19, 20], SILVACO [21, 22], SENTAUROS [23, 24], and SESAME [25, 26]. We decided to use a solar cell capacitance simulator (SCAPS) software, which, despite the limitations and issues described later in this paper, allowed us to perform simulations of the operation

*Corresponding author at: mlabuz@ur.edu.pl

https://doi.org/10.24425/opelre.2026.158736
1896-3757/ Association of Polish Electrical Engineers (SEP) and Polish Academic of Sciences (PAS). Published by PAS

of multi-junction photovoltaic structures based on titanium oxide and copper oxides. It should also be emphasised that this software is the most used and cited solution, which ultimately determined our choice. SCAPS is a one-dimensional solar cell simulator widely used for modelling the electrical behaviour of heterojunction devices under varied physical and environmental conditions. The study evaluates how junction design, material parameters, and layer thicknesses influence cell efficiency and open-circuit voltage (V_{oc}). The results described in the literature indicate that optimisation of these parameters, especially at the heterojunction interface, can significantly improve carrier transport and overall device performance. The findings aim to provide design guidelines and highlight the potential of TiO_2/Cu_xO-based systems as sustainable alternatives for next-generation solar cell technologies.

2. Experimental

2.1. Methods

The present study involves a numerical simulation of both single-junction (n-TiO_2/p-CuO) and tandem (n-TiO_2/p-Cu_xO/n-TiO_2/p-Cu_xO) solar cells using the SCAPS software [27–29]. SCAPS (version 3.3.12), along with supplementary scripts dedicated to multi-junction tandem cells, was applied to calculate key photovoltaic parameters from the current–voltage (J–V) characteristics. Among the evaluated parameters, the short-circuit current density (J_{sc}) and power conversion efficiency (η) under standard test conditions (AM1.5G spectrum, 100 mW/cm², 300 K) were of primary importance.

There are three strategies for studying multi-junction cells, mainly tandem cells, in the SCAPS program [19]. The first is based on calculating generation profiles for the tandem cell and the top and bottom cells. The second one used an additional contact filter containing reflection $R'(\lambda)$ or transmission $T'(\lambda)$ for the top and bottom cells. The last strategy considers both the bottom and top cells, as it encompasses all layers of the tandem cell, but during the calculation, some parts of the cell are replaced with an electronically inactive layer.

In our study, we use the first strategy, i.e., calculation of the generation $G(\lambda, x)$ of electron-hole pairs from the photon flux $N(\lambda, x)$ penetrating the tandem cell. To obtain the number of pairs $G(x)$ generated in unit volume (cm^3) per second for a given spectrum of light, the integration over all wavelengths should be done. The algorithm for this process is implemented in the script provided with SCAPS software. As for other strategies, the calculation is based on splitting the tandem to the top and the bottom cell, but before splitting, the generation profile $G_{tandem}(x)$ is calculated. Then this profile is split into a top-cell profile $G_{top}(x)$ and a bottom-cell profile $G_{bottom}(x)$. These profiles are stored in the files and used for the next steps of the algorithm.

The number of electron-hole pairs generated in the cell is proportional to the number of photons $N(\lambda, x)$ reaching the depth x in the cell:

$$G(x) = \int_{\lambda_{min}}^{\lambda_{max}} \alpha(\lambda, x) N(\lambda, x) d\lambda,$$

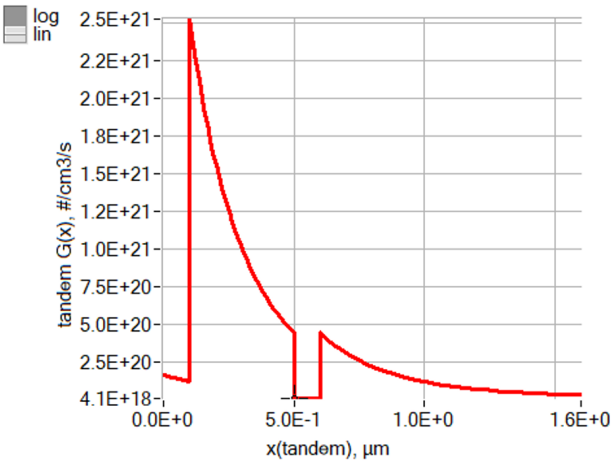

Fig. 1. The generation profile $G(x)$ for a tandem cell of TiO_2/Cu_2O/TiO_2/Cu_2O with a thickness of 0.1/0.4/0.1/1.0 µm, respectively.

where $\alpha(\lambda, x)$ is the absorption constant. The representative shape of $G_{tandem}(x)$ for the tandem cell of $TiO_2/Cu_2O/TiO_2/Cu_2O$ is presented in Fig. 1.

The thicknesses of the individual layers were selected based on insights from previous research [4, 9], while the material properties used in the simulations were obtained from our previous work concerning SCAPS simulations [30]. The specific parameters for TiO_2 and Cu_xO layers used in the simulations are summarised in Table 1.

Table 1.
Parameters of TiO_2, and Cu_xO layers [13].

Material properties	n-TiO_2	p-CuO	p-Cu_2O
Bandgap (eV)	3.2	1.51	2.2
Electron affinity (eV)	4.2	4.07	3.2
Relative dielectric permittivity	10.0	18.1	7.11
CB effective density of states ($1/cm^3$)	$2 \cdot 10^{17}$	$2.2 \cdot 10^{19}$	$2 \cdot 10^{17}$
VB effective density of states ($1/cm^3$)	$6 \cdot 10^{17}$	$5.5 \cdot 10^{20}$	$1.1 \cdot 10^{19}$
Electron mobility (cm^2/Vs)	100	100	200
Hole mobility (cm^2/Vs)	250	0.1	80
Shallow uniform donor density ND ($1/cm^3$)	10^{17}	0	0
Shallow uniform acceptor density NA ($1/cm^3$)	0	10^{16}	10^{18}

2.2. Problem setup

One of the simulated structures of the single and the tandem TiO_2/Cu_xO heterojunction solar cells is illustrated in Fig. 2.

Simulations were performed for different junction designs, layer thicknesses, and optical filters applied to contacts. Among many attempts to obtain the best efficiency, we have applied the SCAPS defined optical filter “95% mirror” (and set it as transmission) for the front contact and “80% mirror” (reflection) for the back contact. For a single junction cell, efficiency increases with increas-

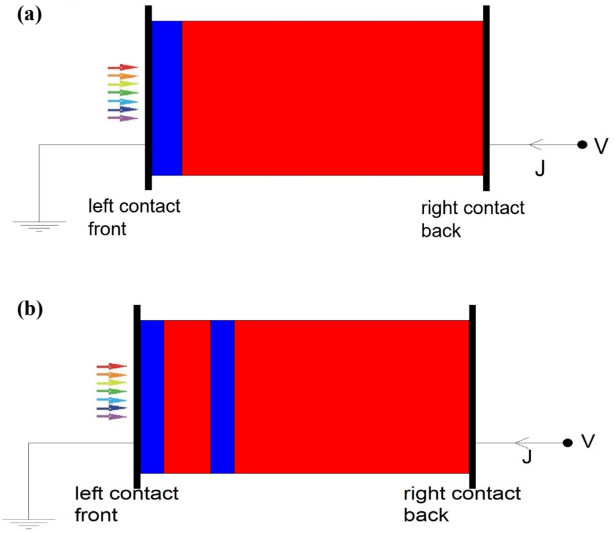

Fig. 2. (a) Single n-TiO_2/p-CuO and (b) tandem n-TiO_2/p-Cu_2O/n-TiO_2/p-CuO heterostructure used in numerical simulations.

ing thickness of p-type layers (Cu_2O or CuO). In Table 2, the parameters for the following "single" cells are presented: n-TiO_2/p-CuO–0.1/2 µm and n-TiO_2/p-Cu_2O–0.1/2 µm.

The configuration for tandem cells is presented in Fig. 2 (b). The calculation procedure for the double layers was carried out according to the following scheme: 1) determining the thickness of the individual layers in tandem, 2) running a script prepared on the basis of the script provided with the SCAPS programme ("test tandem split generation.script"), and 3) changing the thickness of individual layers in order to achieve the best efficiency and repeating the calculation. Only the p-type layers, i.e., Cu_2O and CuO, were changed, because, as our previous simulations showed, they have the greatest influence on the final efficiency of individual cells [30]. Due to the shape of the curve $G(x)$ (see Fig. 1), it was expected that the thickness of the first copper oxide layer (when viewed from the front contact side) should be as thin as possible so that a sufficient number of electron-hole pairs would be generated in the second junction.

To achieve the best efficiencies for tandem cells, a calculation was performed for different thicknesses of the first layer (#1) of copper oxide, taking the thickness of the second layer (#2) of copper as a parameter. The result of the calculations based on the script are graphs showing the individual parameters of the tandem cell, such as: number of electron-hole pairs generated $G(x)$, efficiency of the cell as a function of the R_{back} parameter (%), i.e., reflection from the rear contact, current $J_{sc}(R_{back})$, $V_{oc}(R_{back})$, FF(R_{back}). Figure 4 shows the efficiency obtained for the selected $R_{back} = 80\%$. The explanation of this behaviour of the performance dependence on the thickness of the layers can be based on the dependence $G(x)$, i.e., the number of electron-hole pairs generated as a function of the distance x from the front contact of the tandem cell. The thinner layer #1, the more light reaches the second (counting from the front contact) junction and thus generates a greater number of electron-hole pairs there. However, excessive reduction in the thickness of layer #1 causes the first junction to malfunction. The thickness of the second layer #2 of copper oxide has no such significant impact on the performance of the entire cell as the thickness of the layer #1.

3. Results and discussion

The main parameters of the structures obtained from the simulations are summarised in Table 2. Furthermore, Figure 3 presents the J(V) relation for n-TiO_2/p-Cu_2O and n-TiO_2/p-CuO structures. The best parameters for the single heterojunction were obtained for the TiO_2/CuO structure and we expected even better results for a double heterojunction with TiO_2 and CuO layers. Unfortunately, we were unable to obtain results for the tandem structure of n-TiO_2/p-CuO/n-TiO_2/p-CuO, so we have decided to perform calculations for a double p-type Cu_2O layer and mixed p-type Cu_2O/CuO layers. The best parameters were obtained for the TiO_2/Cu_2O/TiO_2/CuO structure, but the results were worse than in the case of both single structures: TiO_2/Cu_2O, as well as TiO_2/CuO.

Table 2.
J–V characteristics of a single-junction n-TiO_2/p-Cu_xO and a different tandem n-TiO_2/p-Cu_xO/n-TiO_2/p-Cu_xO solar cells (25 °C).

Results	TiO_2/Cu_2O	TiO_2/CuO	TiO_2/Cu_2O/ TiO_2/Cu_2O	TiO_2/Cu_2O/ TiO_2/CuO
Open-circuit voltage, V_{oc} (V)	1.8398	0.8386	8	2.1465
Short-circuit current, J_{sc} (mA/cm^2)	8.5645	26.1522	1.84	5.2895
Fill Factor, FF (%)	65.95	84.96	20	49.39
Efficiency, η (%)	10.39	18.63	3.3	5.61

From the carrier generation profile $G(x)$ shown in Fig. 1, a significant decrease in the number of generated carriers can be observed across the entire thickness of TiO_2 layers #1 and #2. However, the SCAPS numerical procedure fails to converge for TiO_2 layers with a thickness of 0.05 µm, corresponding to half of the thickness used in the single-junction configuration. Moreover, reduced carrier generation in the interconnection region results in a substantial increase in the tandem device series resistance, thereby decreasing the short-circuit current (J_{sc}). It is important to emphasise that the used methodology provides a detailed and physically realistic description of recombination processes, bulk and interfacial defects, as well as charge-carrier transport within each sub-cell, and is therefore well suited for material comparison and the analysis of design trends in tandem device architectures. However, it does not represent a fully self-consistent model of a series-connected tandem device, as it does not explicitly account for the interconnection layers or the recombination junction, nor does it enforce a global current–voltage coupling between the sub-cells. Consequently, the results obtained within this framework should be interpreted as qualitative and comparative rather than as a direct prediction of the absolute electrical characteristics of the complete tandem device.

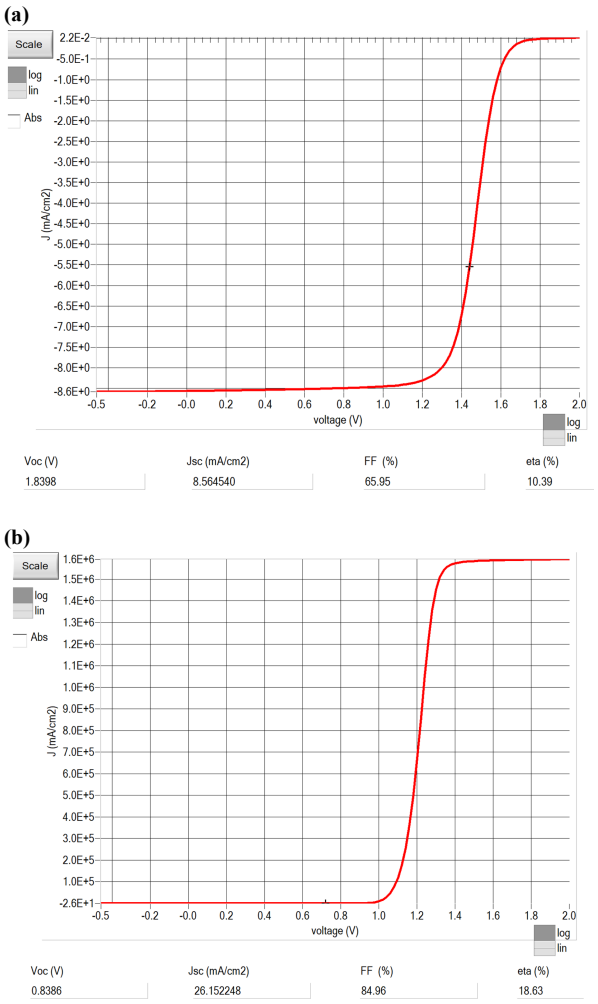

Fig. 3. Current density *vs*. voltage: (a) n-TiO_2/p-Cu_2O structure, (b) n-TiO_2/p-CuO structure.

Figure 4 shows the efficiency of a tandem cell of $TiO_2/Cu_2O/TiO_2/Cu_2O$. The horizontal axis shows the thickness of the first (when viewed from the front contact side) layer of Cu_2O and the thickness of the second layer of Cu_2O is marked with different colours. The grey colour indicates cases where it is not possible to determine the performance. The thicknesses of both titanium oxide layers were 0.1 µm. The data were matched using a function of the form $y = Ae^{-Bx}$ with two parameters: A and B. From Fig. 4, it can be seen that the highest efficiency was achieved for the following thicknesses of copper oxide layers: layer #1: 0.4 µm, layer #2: 1 µm (parameters of tandem are in Table 2). Analysing the graph, we can also see that the efficiency of the tandem cell increases with increasing thickness of the layer #2 and with decreasing thickness of the layer #1. However, once a certain minimum thickness of the layer #1 is exceeded, it is no longer possible to obtain a solution using the method implemented in the script (probably due to numerical problems).

4. Conclusions

TiO_2/Cu_xO photovoltaic cells, due to their structure and the availability of materials, are widely studied worldwide, including by our team. Thanks to buffer layers or annealing,

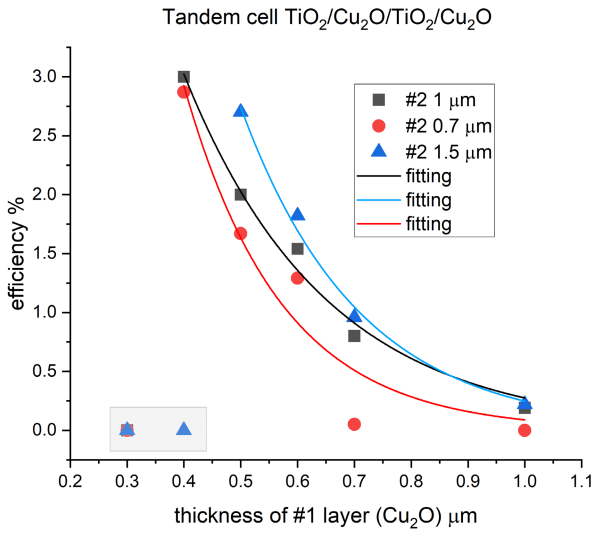

Fig. 4. Efficiency dependence of the $TiO_2/Cu_2O/TiO_2/Cu_2O$ multi-junction on the thickness of Cu_2O layer #1 for various thicknesses of Cu_2O layer #2.

we achieved progressively higher cell efficiency in our previous experiments. To further improve our structures, we used the SCAPS program to simulate both single and tandem TiO_2/Cu_xO structures. Due to the structure and physical processes in the layers, we expected to achieve improvements in the parameters of tandem structures compared to single ones. However, it turned out that the best efficiency was obtained for the n-TiO_2/p-CuO single structure (18.63%), while the best result for the n-TiO_2/p-Cu_2O/n-TiO_2/p-CuO tandem structure was only 5.61%. Unfortunately, it was not possible to perform simulations of tandem n-TiO_2/p-CuO/n-TiO_2/p-CuO cells due to an emerging discrepancy in the numerical calculations.

In contrast, the numerical procedure for the $TiO_2/Cu_2O/TiO_2/Cu_2O$ tandem returns an unexpected value of $V_{oc} \sim 8$ V and an FF of 20% (Table 2), whereas the parameters extracted and calculated directly from the corresponding simulated J–V curve are: $J_{sc} = 1.8$ mA/cm^2, $V_{oc} = 3$ V, FF = 56%, and efficiency $\eta = 3.08\%$.

Difficulties in simulating the properties of tandem systems of photovoltaic cells are also indicated in the SCAPS user manual, where one can find information about the frequent occurrence of convergence in the simulation of more than one number of p-n junctions.

The simulation results obtained in this study differ from those reported in the literature, where multilayer structures typically exhibit an increase in solar cell efficiency. One of the possible explanations of this result are optical losses in the first junction, what is confirmed by reduction of electron-hole pairs generated in the second cell of the tandem. In addition, the applied methodology limitations do not give back a fully self-consistent model of a series-connected tandem device, as it neither explicitly accounts for the interconnection layers nor enforces a global current–voltage coupling between the sub-cells. Therefore, due to the limitations of the SCAPS simulation model, the authors will verify the results both theoretically, by using additional simulation tools and experimentally, by fabricating analogous photovoltaic structures via the magnetron sputtering method.

References

[1] Wojcieszak, D. *et al*. Investigations of structure and electrical properties of TiO_2/CuO thin film heterostructures. *Thin Solid Films* **690**, 137538 (2019). https://doi.org/10.1016/j.tsf.2019.137538

[2] Sawicka-Chudy, P. *et al.* Review of the development of copper oxides with titanium dioxide thin-film solar cells. *AIP Adv.* **10**, 10701 (2020). https://doi.org/10.1063/1.5125433

[3] Hosseini-Sarvari, M., Jafari, F. & Dehghani, A. The study of TiO_2/Cu_2O nanoparticles as an efficient nanophotocalyst toward surface adsorption and photocatalytic degradation of methylene blue. *Appl. Nanosci.* **12**, 2195–2205 (2022). https://doi.org/10.1007/s13204-022-02474-x

[4] Wisz, G. *et al*. Impact of titanium and copper buffer layers on the structure and I-V characteristics of TiO_2/Cu_xO thin film solar cells. *Appl. Surf. Sci.* **682**, 161650 (2025). https://doi.org/10.1016/j.apsusc.2024.161650

[5] Salgado-Conrado, L., Álvarez-Macías, C. & Reyes-Durán, B. A review of simulation tools for thin-film solar cells. *Materials* **17**, 5213 (2024). https://doi.org/10.3390/ma17215213

[6] Kowsar, A. *et al*. An overview of solar cell simulation tools. *Sol. Energy Adv.* **5**, 100077 (2025). https://doi.org/10.1016/j.seja.2024.100077

[7] Wisz, G. *et al*. Formation and characterization of stable TiO_2/Cu_xO-based solar cells. *Materials* **16**, 5683 (2023). https://doi.org/10.3390/ma16165683

[8] Ciria-Ramos, I., Juarez-Perez, E. J. & Haro, M. Solar energy storage using a Cu_2O-TiO_2 photocathode in a lithium battery. *Small* **19**, 2301244 (2023). https://doi.org/10.1002/smll.202301244

[9] Wisz, G. *et al*. Effect of annealing in air on the structural and optical properties and efficiency improvement of TiO_2/Cu_xO solar cells obtained via direct-current reactive magnetron sputtering. *Materials* **18**, 888 (2025). https://doi.org/10.3390/ma18040888

[10] Enebe, G. C., Ukoba, K. & Jen, T.-C. Numerical modeling of effect of annealing on nanostructured CuO/TiO_2 pn heterojunction solar cells using SCAPS. *AIMS Energy* **7,** 527–538 (2019). https://doi.org/10.3934/energy.2019.4.527

[11] Gray, J. L. *et al*. ADEPT 2.1 https://nanohub.org/resources/10913?rev=151 (2015). (access: Nov. 26th, 2025).

[12] Gray, J. L. ADEPT: A General Purpose Numerical Device Simulator for Modeling Solar Cells in One-, Two-, And Three-Dimensions. in *Proceedings of the Twenty-Second IEEE Photovoltaic Specialists Conference 1991* **1**, 436–438 (1991). https://doi.org/10.1109/PVSC.1991.169253

[13] Stangl, R., Leendertz, C. & Haschke, J. Numerical Simulation of Solar Cells and Solar Cell Characterization Methods: The Open-Source on Demand Program AFORS-HET. in *Solar Energy* (ed. Rugescu, R. D.) 319–354 (InTechOpen, 2010). https://doi.org/10.5772/8073

[14] Aydin, B. Photovoltaic investigation of diamane emitter layer with AFORS-HET. *Opt. Laser Technol.* **186**, 112696 (2025). https://doi.org/10.1016/j.optlastec.2025.112696

[15] Liu, Y., Heinzel, D. & Rockett, A. A Revised Version of the AMPS Simulation Code. in *Proceedings of the 35th IEEE Photovoltaic Specialists Conference* 1943–1947 (IEEE, 2010). https://doi.org/10.1109/PVSC.2010.5616225

[16] Al-shamiri, H .A. S., Sid-Ahmed, M. O. & Abdu Hezam, F. Simulation of performance of cadmium telluride solar cell using AMPS-1D program. *J. Photonic Mater. Technol.* **2**, 14–19 (2016). https://doi.org/10.11648/j.jmpt.20160202.11

[17] PC1Dmod6.1 User Manual https://www2.pvlighthouse.com.au/resources/PC1D/PC1Dmod6/PC1Dmod%206-1%20help.pdf (access: Nov. 26th, 2025).

[18] Humaidan, R. M., Dahham, A. T. & Majeed, Z. N. Designed and simulation of AlGaAs: GaAs thin film solar cell using PC1D program. *NeuroQuantology* **20**, 265–270 (2022). https://doi.org/10.14704/nq.2022.20.3.NQ22254

[19] Burgelman, M. *et al*. *SCAPS Manual*. (University of Gent, 2025). https://scaps.elis.ugent.be/SCAPS%20manual%20most%20recent.pdf (access: Nov. 26th, 2025).

[20] Lotfy, L. A. *et al*. Numerical simulation and optimization of FTO/TiO_2/CZTS/CuO/Au solar cell using SCAPS-1D. *Sci. Rep.* **15**, 28022 (2025). https://doi.org/10.1038/s41598-025-12999-0

[21] Silvaco TCAD Solution https://silvaco.com/tcad (access: Nov. 26th, 2025).

[22] Dogra, S. & Kumar, V. Implementation of Organic Thin Film Transistor Using Silvaco TCAD. in *2025 International Conference on Electronics, AI and Computing (EAIC)* 1–4 (2025). https://doi.org/10.1109/eaic66483.2025.11101383

[23] Sentaurus Device *Synopsys* https://www.synopsys.com/manufacturing/tcad/device-simulation/sentaurus-device.html (access: Nov. 26th, 2025).

[24] Wu, Y.-C. & Jhan, Y.-R. Introduction of Synopsys Sentaurus TCAD Simulation. in: *3D TCAD Simulation for CMOS Nanoeletronic Devices*. (Springer, Singapore, 2018). https://doi.org/10.1007/978-981-10-3066-6_1

[25] SESAME description *NIST* https://pages.nist.gov/sesame/ (access: Nov. 26th, 2025).

[26] Gaury, B., Sun, Y., Bermel, P. & Haney, P. Sesame: A 2-dimensional solar cell modeling tool. *Sol. Energy Mater. Sol. Cells* **198**, 53–62 (2019). https://doi.org/10.1016/j.solmat.2019.03.037

[27] Ait-Wahmane, Y. *et al*. Comparison study between ZnO and TiO_2 in CuO based solar cell using SCAPS-1D. *Mater. Today: Proc.* **52**, 166–171 (2022). https://doi.org/10.1016/j.matpr.2021.11.535

[28] Das, M. M., Panda, S. & Mohapatra, N. Role of La_2CuO_4 as buffer layer for a significant improvement of the performance of TiO_2/Cu_2O based all-oxide solar cell: A SCAPS-1D numerical analysis. *Adv. Theory Simul.* **8**, 2400565 (2024). https://doi.org/10.1002/adts.202400565

[29] Jahan, N. *et al*. A comparative study of CuO based solar cell with ZnTe HTL and SnS_2 ETL using SCAPS 1D simulation. *J. Opt.* **54**, 952–964 (2024). https://doi.org/10.1007/s12596-024-01800-6

[30] Sawicka-Chudy, P. *et al*. Simulation of TiO_2/CuO solar cells with SCAPS-1D software. *Mater. Res. Express* **6**, 085918 (2019). https://doi.org/10.1088/2053-1591/ab22aa